Title
Modes of Elliptical Waveguides; a Correction

Authors
Goldberg, D.A.
Laslett, L.J.
Rimmer, R.A.

Publication Date
1990-03-01

LBL-28702
UC-411

Lawrence Berkeley Laboratory
UNIVERSITY OF CALIFORNIA

Accelerator & Fusion Research Division

Modes of Elliptical Waveguides; a Correction

D.A. Goldberg, L.J. Laslett, and R.A. Rimmer

March 1990

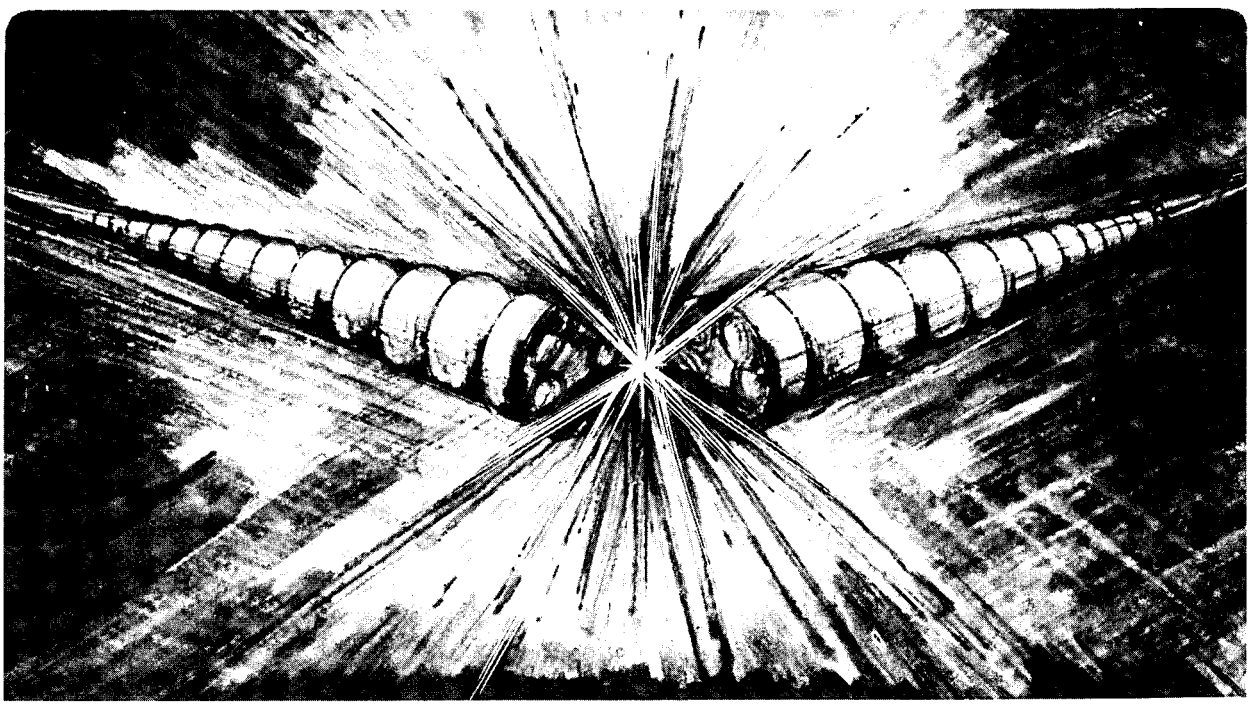

Prepared for the U.S. Department of Energy under Contract Number DE-AC03-76SF00098.

DISCLAIMER

MODES OF ELLIPTICAL WAVEGUIDES; A CORRECTION

D.A. Goldberg, L.J. Laslett, and R.A. Rimmer
*Lawrence Berkeley Laboratory, Berkeley, CA 94720**

We show that the fields associated with the TM_{01} mode of an elliptical wave guide are qualitatively different from those which have appeared in the standard literature for the past fifty years, and that the original fields as plotted were also in qualitative disagreement with the analytic expressions which accompanied them. Nonetheless, the cutoff frequencies given for that mode, as well as for the five other modes described in those references, are exceedingly accurate (within roughly 1%) for elliptical eccentricities as large as 0.75; for eccentricities in excess of 0.9, the inaccuracy increases to from 5 to nearly 50%, depending on the mode in question.

1. Introduction

The analytic solutions for the lowest modes of an elliptical waveguide were first published some fifty years ago in a classic paper by L-J Chu [1]; references published as recently as 1986 [2] make use of Chu's original expressions and figures. In the course of checking the accuracy of a numerical field solver by using it to determine the cutoff frequencies of an elliptical waveguide, we observed that while the field solver yielded a cutoff frequency for the TM_{01} mode which was quite close to that shown in Refs. 1 and 2, it predicted a field pattern which was strikingly at variance with that shown in those references. The former gave a field pattern that was basically a deformed version of the TM_{01} mode for the circular guide (having a single, on-axis "flux tube" of E_z); the latter's solution showed a *pair* of E_z flux tubes, pointing in the *same direction*, located at what appeared to be the foci of the ellipse (see Fig. 1 below). Upon further examination, it appeared that the field pattern depicted in Refs. 1 and 2 was at variance with the analytic expressions contained in those same references.

We decided that the most direct approach to resolving the above discrepancies would be to solve the wave equation by numerical integration, using an iterative technique to obtain the relevant eigenvalues. To give away the show at the outset, we wound up concluding that indeed the fields shown for the TM_{01} mode in Refs. 1 and 2 were qualitatively incorrect, and that the error had apparently gone undetected for some five decades.

In the course of obtaining our solutions to this problem, and of examining the discrepancies between the analytic expressions and field plots in Refs. 1 and 2, we managed to demystify for ourselves both the Mathieu equation and its solutions, as well as the elliptical coordinate system. In the hope of being able to render a similar service to our readers, we elected to report our results in the present, somewhat expanded form, rather than simply submitting them as a one-line (or more accurately, one-figure) erratum.

2. The Wave Equation in Elliptical Coordinates

For a cylindrical waveguide (i.e. of constant cross-section), the z-dependence of the electric and magnetic fields is simply given by $e^{-jk_z z}$. Hence for TM (TE) waves, the wave equation for the longitudinal component of the electric (magnetic) field takes the form

* Work supported by the Director, Office of Energy Research, Office of High Energy and Nuclear Physics, High Energy Physics Division, U.S. D.O.E., under Contract No. DE-AC03-76SF00098.

$$\nabla_\perp^2 \begin{Bmatrix} E_z \\ H_z \end{Bmatrix} + (k^2 - k_z^2) \begin{Bmatrix} E_z \\ H_z \end{Bmatrix} = 0 \tag{1}$$

where $\nabla_\perp^2$ represents the two-dimensional (i.e. in the transverse plane) Laplacian, and k is the wave number (ω/c) in unbounded space.

For a waveguide whose cross section is of the form of an ellipse of focal distance ρ, it is convenient to use confocal elliptical coordinates (see Appendix). In this system, Eq. 1 can be rewritten as [3]

$$\frac{2}{\rho^2 (\cosh 2\xi - \cos 2\eta)} \left(\frac{\partial^2}{\partial \xi^2} + \frac{\partial^2}{\partial \eta^2} \right) \begin{Bmatrix} E_z \\ H_z \end{Bmatrix} + (k^2 - k_z^2) \begin{Bmatrix} E_z \\ H_z \end{Bmatrix} = 0 \tag{2}$$

Assuming that E_z (H_z) can be written in the form $U(\xi) \cdot V(\eta)$ [$\cdot e^{-jk_z z}$], we can rewrite Eq. 2 as

$$\frac{1}{U} \frac{\partial^2 U}{\partial \xi^2} + \frac{k^2 - k_z^2}{2} \rho^2 \cosh 2\xi = -\frac{1}{V} \frac{\partial^2 V}{\partial \eta^2} + \frac{k^2 - k_z^2}{2} \rho^2 \cos 2\eta \tag{3}$$

where by the usual argument, the left- and right-hand sides of Eq. 3 must be equal to a separation constant, which in accordance with conventional usage we define as a (not to be confused with the semi-major axis of the ellipse). We can then rewrite Eq. 3 as two separate equations

$$\frac{d^2 U}{d\xi^2} - (a - 2q \cosh 2\xi)\, U = 0 \tag{4a}$$

$$\frac{d^2 V}{d\eta^2} + (a - 2q \cos 2\eta)\, V = 0 \tag{4b}$$

where, according to standard usage [3,4] we have defined

$$q \equiv \frac{k^2 - k_z^2}{4} \rho^2 \tag{5}$$

Equation 4b for the "angular" dependence is the Mathieu equation; Eq. 4a, which gives the "radial" dependence, is usually known as the modified Mathieu equation. Because both separation constants, a and q, appear in both equations, the solutions are more properly written as $V(a,q;\eta)$ and $U(a,q;\xi)$, respectively

We are now in a position to write down formally the solutions to Eq. 3. If we define

$$W(\xi,\eta) \equiv U(\xi) \cdot V(\eta)$$

then for TM modes (E waves), W describes the ξ,η-dependence of the E_z field; it must satisfy the boundary condition $U(\xi_o) = 0$, where ξ_o is the radial coordinate of the ellipti-

cal boundary. For TE modes (H-waves), W describes the H_z field, and satisfies the boundary condition $U'(\xi_o) = 0$.

In the usual fashion, one can obtain the transverse field components from the longitudinal field. Shown below are the relevant relations for elliptical coordinates; essentially these are the equations appearing in Refs. 1 and 2, albeit with slightly different notation. In all cases a z-dependence of $e^{-jk_z z}$ is understood; for completeness, we include the z-fields explicitly.

TE Modes: TM Modes

$$H_z = A\,U(\xi)\,V(\eta) \qquad E_z = A\,U(\xi)\,V(\eta) \tag{6a,b}$$

$$H_\xi = -\frac{E_\eta}{Z_{TE}} = -\frac{j\,k_z\,A\,U'(\xi)\,V(\eta)}{\rho_1\,(k^2 - k_z^2)} \qquad E_\xi = Z_{TM} H_\eta = -\frac{j\,k_z\,A\,U'(\xi)\,V(\eta)}{\rho_1\,(k^2 - k_z^2)} \tag{7a,b}$$

$$H_\eta = \frac{E_\xi}{Z_{TE}} = -\frac{j\,k_z\,A\,U(\xi)\,V'(\eta)}{\rho_1\,(k^2 - k_z^2)} \qquad E_\eta = -Z_{TM} H_\xi = -\frac{j\,k_z\,A\,U(\xi)\,V'(\eta)}{\rho_1\,(k^2 - k_z^2)} \tag{8a,b}$$

where

$$Z_{TE} = \frac{\mu\omega}{k_z} = \frac{Z_o}{\sqrt{1 - (\omega_c/\omega)^2}} \qquad Z_{TM} = \frac{k_z}{\varepsilon\omega} = Z_o\sqrt{1 - (\omega_c/\omega)^2} \tag{9a,b}$$

and

$$\rho_1 = \rho\sqrt{\cosh^2\xi - \cos^2\eta} = \rho\sqrt{\sinh^2\xi + \sin^2\eta} \tag{10}$$

2.1 Solutions to the Wave Equation and their Properties

We adopt the notation of Refs. 3 and 4 and denote the $V(a,q;\eta)$ which satisfy the required periodic boundary conditions as $\mathrm{se}_m(q;\eta)$ and $\mathrm{ce}_m(q;\eta)$, depending on whether the function or its derivative is zero at $\eta = 0, 2\pi$. The constant m turns out to be equal to the number of nodes in the interval $0 \le \eta < \pi$; in this notation m has effectively replaced a as the second separation constant. In like manner, the two radial solutions are defined as $\mathrm{Se}_m(q;\xi)$ and $\mathrm{Ce}_m(q;\xi)$.

Looking at the full solution, we note that there are two different kinds of $W(\xi,\eta)$, namely

$$W(\xi,\eta) = \mathrm{Ce}_m(q;\xi)\,\mathrm{ce}_m(q;\eta) \tag{11a}$$

$$W(\xi,\eta) = \mathrm{Se}_m(q;\xi)\,\mathrm{se}_m(q;\eta) \tag{11b}$$

sometimes referred to as even and odd solutions, respectively. Although it might seem initially that all combinations of the Ce, Se, ce, and se would be possible, it is shown in Ref. 4 that continuity of both W and its vertical gradient across the interfocal line $\xi = 0$ restricts the allowed combinations to the two shown.

2.2. Calculation of Eigenfrequencies

Of comparable importance to the field distributions are the frequencies of the various eigenmodes. The most direct method of calculating these frequencies is by numerical integration of Eqs. 4a and 4b. Because both separation constants appear in both equations, one must solve for both sets of eigenvalues simultaneously, by what amounts to a double iteration method, looking for combinations of a and q, which simultaneously satisfy the angular and radial boundary conditions. Having obtained the q (along with the a, or equivalently, the m) for a given mode, one can use Eq. 5 to obtain the mode frequency. Using the same convention as conventionally applied to the modes for a circular geometry, we label them with the indices mr, with m, the index of the angular Mathieu function, indicating the number of oscillations between 0 and 2π, and r indicating that the radial solution corresponds to the rth root (i.e. value of q) of $U_m(q;\xi_o) = 0$ (for TM modes) or of $U_m'(q;\xi_o) = 0$ (for TE modes). In this notation,

$$f_{mr} = \frac{k_{mr}\, c}{2\,\pi} = \frac{c}{2\,\pi}\sqrt{\frac{4\,q_{mr}}{\rho^2} + k_z^2} \tag{12a}$$

For a cylindrical cavity of length ℓ, k_z is $n\pi/\ell$, where n is the number of longitudinal half-waves; for a wave guide, its value is unrestricted. In fact Eq. 12a can be used to find the cutoff frequency of the mr mode by setting $k_z = 0$, whereupon we have

$$f_{mr}^{cutoff} = \frac{c}{\pi\,\rho}\sqrt{q_{mr}} \tag{12b}$$

Chu's [1] method of arriving at the value of q_{mr} was somewhat similar. However, rather than numerically integrating the radial equation, Chu used Fourier-Bessel expansions of the Ce_m and Se_m, based on (at that time) unpublished M.I.T. tables. Starting with a given value of $k\rho$ (equivalent to assuming a q; see Eq. 5), he then calculated by successive approximation the value of ξ_o (or equivalently the eccentricity e–see Appendix) for which the appropriate radial boundary conditions were satisfied, always restricting himself to the lowest radial root ($r = 1$); operationally this amounted to determining $e(q)$ rather than $q(e)$. In this way he could obtain a set of "universal" curves by plotting for each mode the dimensionless quantity $k\rho$ as a function of e. Because of the specific problem he was considering, Chu instead chose the equivalent device of scaling the cutoff wavelength $\lambda_o = 2\pi/k$ to the circumference of the ellipse. That quantity is given by

$$s = 4\rho/e\ \ \mathsf{E}(e) \tag{13}$$

where $\mathsf{E}(e)$ (sometimes written as $\mathsf{E}(\sin\alpha)$ or simply–and ambiguously–$\mathsf{E}(\alpha)$) is the complete elliptic integral of the second kind. It then follows that

$$\frac{\lambda_o}{s} = \frac{\pi e}{4\mathsf{E}(e)\,\sqrt{q}} = \frac{\pi e}{2\mathsf{E}(e)\,k\rho} \tag{14}$$

Having performed this procedure for the six lowest modes, Chu presumably interpolated on these curves (so as to get the appropriate q) to be able to calculate the fields for the case $e = 0.75$, the plots of which are presented in his paper, and referred to in Ref. 2.

3. Comparison of Results

We compare the eigenmodes obtained using our numerical integration technique (Method 1) with those obtained by Chu in Ref. 1 (Method 2) for two different ellipses: The first is an ellipse of semi-axes 10 and 6.614 cm, corresponding to an e of 0.75; this is the case for which the field plots are presented in Ref. 1. The second is an ellipse of semi-axes of 6 and 2 cm , corresponding to an e of .94281; this is the geometry of the waveguide (actually an accelerator beam tube) we were working on when this problem originally arose.

Table 1: Cutoff frequencies for the six lowest modes of an elliptical wave guide.

MODE	FREQUENCY (GHz)			
	e = 0.75		e = 0.9428	
	Method 1	Method 2	Method 1	Method 2
EVEN TE_{11}	.889	.88	1.496	1.457
ODD TE_{11}	1.300	1.30	4.095	4.31
EVEN TM_{01}	1.467	1.46	4.205	4.49
EVEN TM_{11}	2.124	2.11	5.11	5.91
EVEN TE_{01}	2.500	2.64	7.876	12.5
ODD TM_{11}	2.554	2.64	7.92	12.5

Comparison of the first two columns shows that Chu's results (Method 2) are extremely accurate for the case of e =.75 (discrepancies here may simply be attributable to the accuracy with which one can read the values from the published curves). The reduced accuracy for the higher eccentricity, particularly the higher-frequency modes, is at least partly attributable to the fact that Chu is plotting the *wavelength*, rather than the frequency, and since the frequency for the higher modes increases with increasing eccentricity, a given reading error translates into a larger percentage error in the frequency; notwithstanding this consideration, the "exact" solutions (Method 1) clearly lie off Chu's curves for the higher eccentricity. This would suggest that the accuracy of either the tables or the truncated expansions used by Chu decreases in the limit of large q and small ξ.

Perhaps more striking than the agreement in frequency for the modes of the $e = 0.75$ ellipse is the fact that the figure presented for the fields of the even TM_{01} (or ${}_eE_o$) mode, shown in Fig. 1, reproduced from Ref. 1, are *qualitatively incorrect* (this *despite* the fact that the cutoff frequency for this mode is correctly calculated in Ref. 1!). This can be seen in several ways.

Fig. 1 shows a reversal in the sign of E_x as x increases. However as we shall now show, this is incompatible with Eqs. 7b and 8b for the TM_{01} mode. We begin by noting that for points on the x-axis to the right of $x = \rho$, $E_x = E_\xi$. Also, for these points $\eta = 0$, so that, from Eq. 7b we have

$$E_x(\xi,0) = -\frac{j\,k_z\,A\,U'(\xi)\,V(0)}{(k^2-k_z^2)\,\rho_1(\xi,0)} = C\,\frac{U'(\xi)\,V(0)}{\sinh\xi} \qquad (15a)$$

Similarly, for point on the interfocal line to the left of $x = \rho$, $E_x = -E_\eta$, and $\xi = 0$, so that from Eq. 8b we have

$$E_x(0,\eta) = -C\frac{U(0)\,V'(\eta)}{\sin\eta} \tag{15b}$$

where the constant in Eq. 15b is the same as that in Eq. 15a. For the case of the TM_{01} mode, $U(\xi)$ and $V(\eta)$ are $Ce_0(\xi)$ and $ce_0(\eta)$, respectively.

Eqs. 15a and 15b show that the relative signs of E_x on either side of the focus depend on the relative signs of $Ce_0'(\xi)$ and $ce_0'(\eta)$. We have plotted these functions in Figs. 2 and 3, respectively, for the case of an ellipse with $e = 0.75$ and with a q corresponding to the cutoff frequency of its TM_{01} mode. From Fig. 2, we see that the sign of $Ce_0'(\xi)$ is everywhere negative; from Fig. 3, that the sign of $ce_0'(\eta)$ is positive throughout the region $0 \le \eta \le \pi/2$. (In fact, both these results are true for *any* positive value of q, provided the radial function has its first zero at the outer boundary.) Hence, from Eqs. 15a and 15b, we see that the sign of E_x is the same for all positive x, in direct contradiction to the figure.

We should note that it might appear from the presence of the ρ_1 term in the denominators of Eqs. 7 and 8 that there is some sort of singularity in the transverse fields just at the points $\xi = 0$; $\eta = 0, \pi$, i.e., the foci of the ellipses; we will now show that this is not the case. In our discussion we will consider only the horizontal E-field at the right hand focus for the case of the TM modes; the arguments can easily be extended to all other cases.

In the immediate neighborhood of $x = \rho$, we can approximate $\sinh\xi$ by ξ, $\sin\eta$ by η, $U'(\xi)$ by $U''(0)\,\xi = (a - 2q\cosh 2\xi)\,U(0)\,\xi$, and $V'(\eta)$ by $V''(0)\,\eta = (-a + 2q\cos 2\eta)\,V(0)\,\eta$, whereby we find that

$$\lim_{\xi\to 0} E_x(\xi,0) = \lim_{\eta\to 0} E_x(0,\eta) = (a - 2q)\,C\,U(0)\,V(0) \tag{16}$$

From Eq. 16 we see that E_x is both finite and continuous at the point $(\xi,\eta) = (0,0)$.

It might appear that this result would admit of a sign change in E_x in the event that either $U(0)$ or $V(0)$ were zero at this point. For the particular case of the TM_{01} mode, neither function exhibits this behavior. More generally, from Eqs. 11a and 11b we see that it is only the odd solutions which admit of this behavior; in fact for those solutions, *both* $U(0)$ and $V(0)$ are zero, thereby requiring that E_x be zero everywhere along the x-axis.

Since the transverse fields are derivable from the longitudinal fields, we might also expect a contradiction to arise with respect to E_z, and this is in fact the case. Figure 1 suggests that the value of E_z on the x-axis initially increases with x, reaching a maximum at a point which appears to be the focus of the ellipse (although the point is not explicitly identified as such in Ref. 1); in elliptical coordinates this would correspond to η decreasing from $\pi/2$ to 0 (see Fig. A.1 in the appendix). However, as shown in Fig. 3, ce_0 is a *maximum* at $\eta = \pi/2$, meaning that E_z decreases with increasing x. In fact, similar to the result for the transverse field, this angular dependence of E_z characterizes not only this particular TM_{01} mode, but rather *any* $m = 0$ mode (for *any* positive q, and hence any eccentricity).

Before presenting a correct version of Fig. 1, we describe briefly the procedure used to obtain the field lines for the E and H fields. For a TM mode, E_z is proportional to the vector potential for the (transverse) H field. Hence, lines of constant E_z are field lines of H, and uniform spacing of contours of constant E_z results in a line density proportional to the value of the local H field; such contours can be readily obtained by taking the (previously obtained) numerical solutions to Eqs. 4a and 4b, and substituting them into Eq. 6b.

Obtaining the E fields is somewhat more difficult. The E-field lines are characterized by the relation

$$\frac{d\eta}{d\xi} = \frac{E_\eta}{E_\xi} \tag{17}$$

From Eqs. 7b and 8b, we have that

$$\frac{E_\eta}{E_\xi} = \frac{U(\xi)\, V'(\eta)}{U'(\xi)\, V(\eta)} \tag{18}$$

We can evaluate the right-hand side of Eq. 18 by numerically integrating Eqs. 4a and 4b starting at the outer boundary, using the initial values for U, U', V, and V' obtained from the previously obtained numerical solutions of Eqs. 4a and 4b, "simultaneously" substituting this result into Eq. 17 and integrating to obtain $\eta(\xi)$. To choose the starting η values to produce a line density proportional to the field strength, we note from Eqs. 7b and A.6 (see Appendix) that the flux of the electric field on the outer boundary is given by

$$\int E_\xi \, ds \propto \int V(\eta)\, d\eta \tag{19}$$

Hence, we need merely choose the values of η to obtain equal increments in the integral of $V(\eta)d\eta$, a quantity we can calculate by numerically integrating the previously obtained solutions to Eq. 4b.

The true appearance of the electric field for the TM_{01} mode is as shown in Fig. 4, essentially a deformed version of the corresponding mode for a circular guide, a result which holds for all values of q and e. This result, although not particularly surprising, is by no means a universal occurrence. In particular, as far as bifurcation of flux tubes is concerned, this can indeed occur in the transition between circular and elliptic geometries, although it generally happens in the *reverse* sense: For example, for the even TM_{m1} modes with $m > 1$, what are single flux tubes in moderately eccentric elliptical geometry can bifurcate as the geometry becomes more nearly circular.

It is perhaps a fruitless endeavor to speculate on the origin of the erroneous field plot in Ref. 1; however, one cannot help but conjecture. The most likely (and, in our view, the only plausible) explanation is that when the fields were calculated, the values of $ce_0(q;\eta)$ used to generate the fields were, for one reason or other, those corresponding to a *negative* q, albeit with the correct magnitude (the values of $Ce_0(q;\xi)$ would still have had to be calulated correctly). This would have interchanged the nature of the extrema at $\eta = 0$ and $\pi/2$ and reversed the relative field directions on either side of the foci, consistent with the field plots in Ref. 1.

Acknowledgements

This work was largely stimulated by G.R. Lambertson's suggestion that the solution for the TM_{01} mode pictured in Refs. 1 and 2 seemed to be incorrect. Discussions of this problem with D. L. Judd have been both stimulating and informative.

References

1. Chu, Lan-Jen, "Electromagnetic Waves in Elliptic Hollow Pipes of Metal," J. Appl. Phys. **9**, 583 (1938).
2. Marcuvitz, N., *Waveguide Handbook*, (Peter Peregrinius, London, 1986), pp. 80-84.
3. Blanch, G., in *Handbook of Mathematical Functions*, edited by M. Abramowitz and I.A. Stegun (Dover, New York, 1972), p. 722
4. McLachlan, N.W., *Theory and Application of Mathieu Functions,* (Clarendon, Oxford, 1947).
5. See Ref. 4; p.236.

APPENDIX: ELLIPTICAL CO-ORDINATES

The elliptical coordinate system uses as the "radial" coordinate ξ a set of confocal ellipses, with the orthogonal coordinate η being a set of hyperbolas having the same foci (see Figure A.1). The quantity ξ is defined by the relation

$$\xi \equiv \cosh^{-1}(a/\rho) \tag{A.1}$$

where ρ is the focal distance of the ellipse, and is related to the semi-major and semi-minor axes by

$$\rho = \sqrt{a^2 - b^2} \tag{A.2}$$

The relation between elliptical and cartesian coordinates is given by

$$x = \rho \cosh \xi \cos \eta \qquad\qquad y = \rho \sinh \xi \sin \eta \tag{A.3a,b}$$

It is frequently useful to parametrize an ellipse in terms of its eccentricity e defined by

$$e = \rho/a \tag{A.4}$$

whence we can rewrite Eq. A.1 as

$$\xi = \cosh^{-1}(1/e) \tag{A.5}$$

Finally, from Eqs. A.3a,b we can obtain the expression for the differential path length in elliptical coordinates

$$ds = \rho \sqrt{(\cosh^2\xi - \cos^2\eta)\,(d\xi^2 + d\eta^2)} \tag{A.6}$$

FIGURE CAPTIONS

Figure 1. Field pattern for the TM_{01} mode for an ellipse of $e = 0.75$, as shown in Ref. 1. Solid lines represent the electric field; dashed lines, the magnetic. Both the implied initial increase in E_z and the change of sign of E_z with increasing x are inconsistent with the analytic expression for the field (see text).

Figure 2. Radial dependence of E_z for the TM_{01} mode for an ellipse with $e = 0.75$, i.e. a plot of $Ce_0(q;x)$ for the q corresponding to the aforementioned mode.

Figure 3. Angular dependence of E_z for the TM_{01} mode for an ellipse with $e = 0.75$, i.e. a plot of $ce_0(q;x)$ for the q corresponding to the aforementioned mode.

Figure 4. Field pattern for the TM_{01} mode for an ellipse of $e = 0.75$, obtained from the numerically integrated solutions, as described in the text; the field-line conventions are the same as in Fig. 1.

Figure A.1. The elliptical coordinate system.

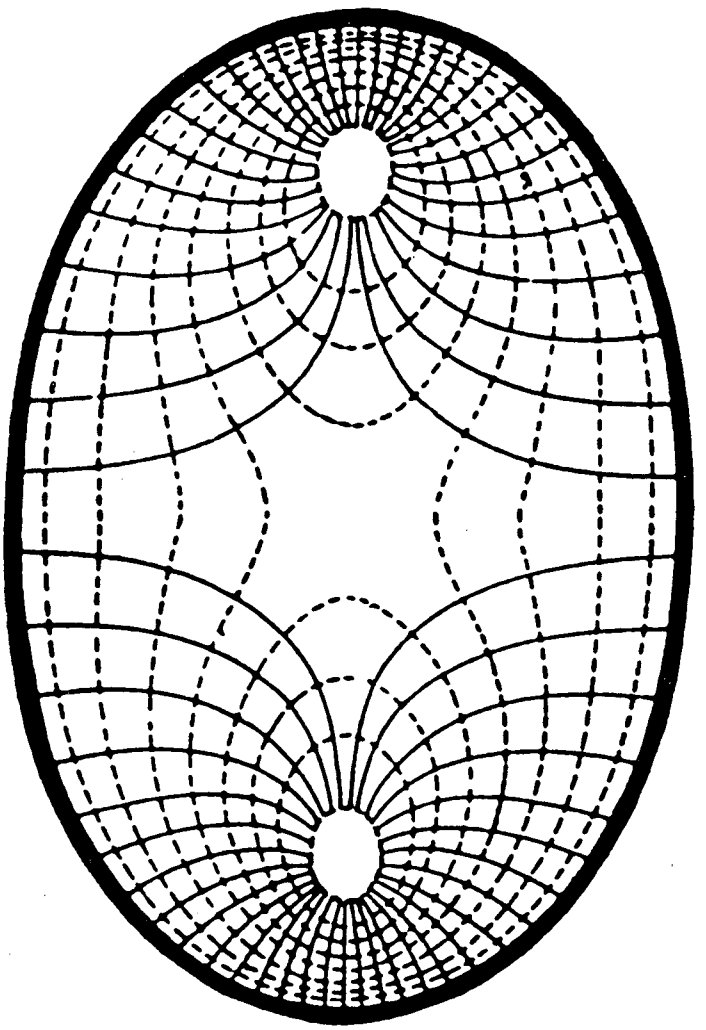

Figure 1

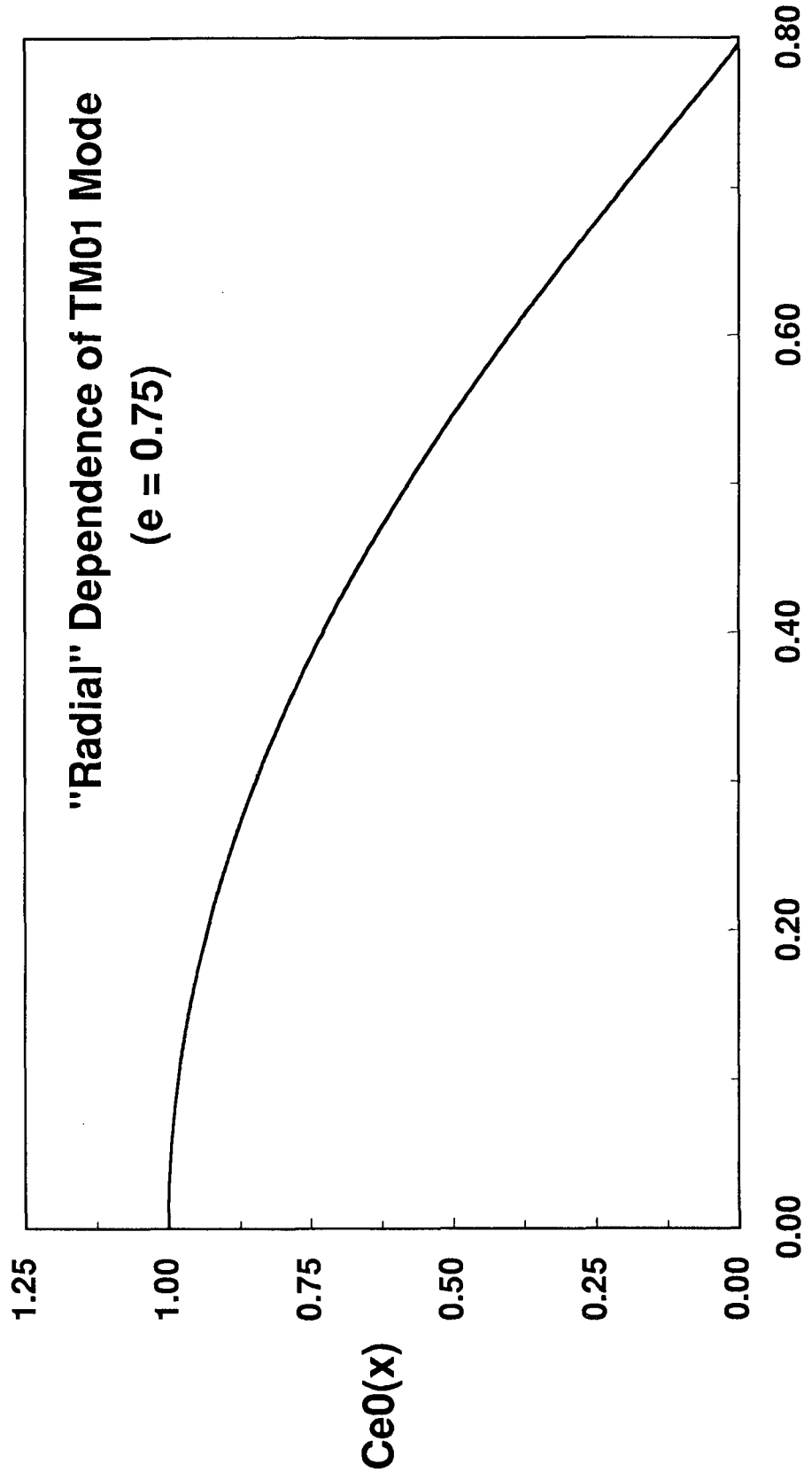
"Radial" Dependence of TM01 Mode
(e = 0.75)
Ce0(x)
1.25
1.00
0.75
0.50
0.25
0.00
0.00
0.20
0.40
0.60
0.80
x

Figure 2

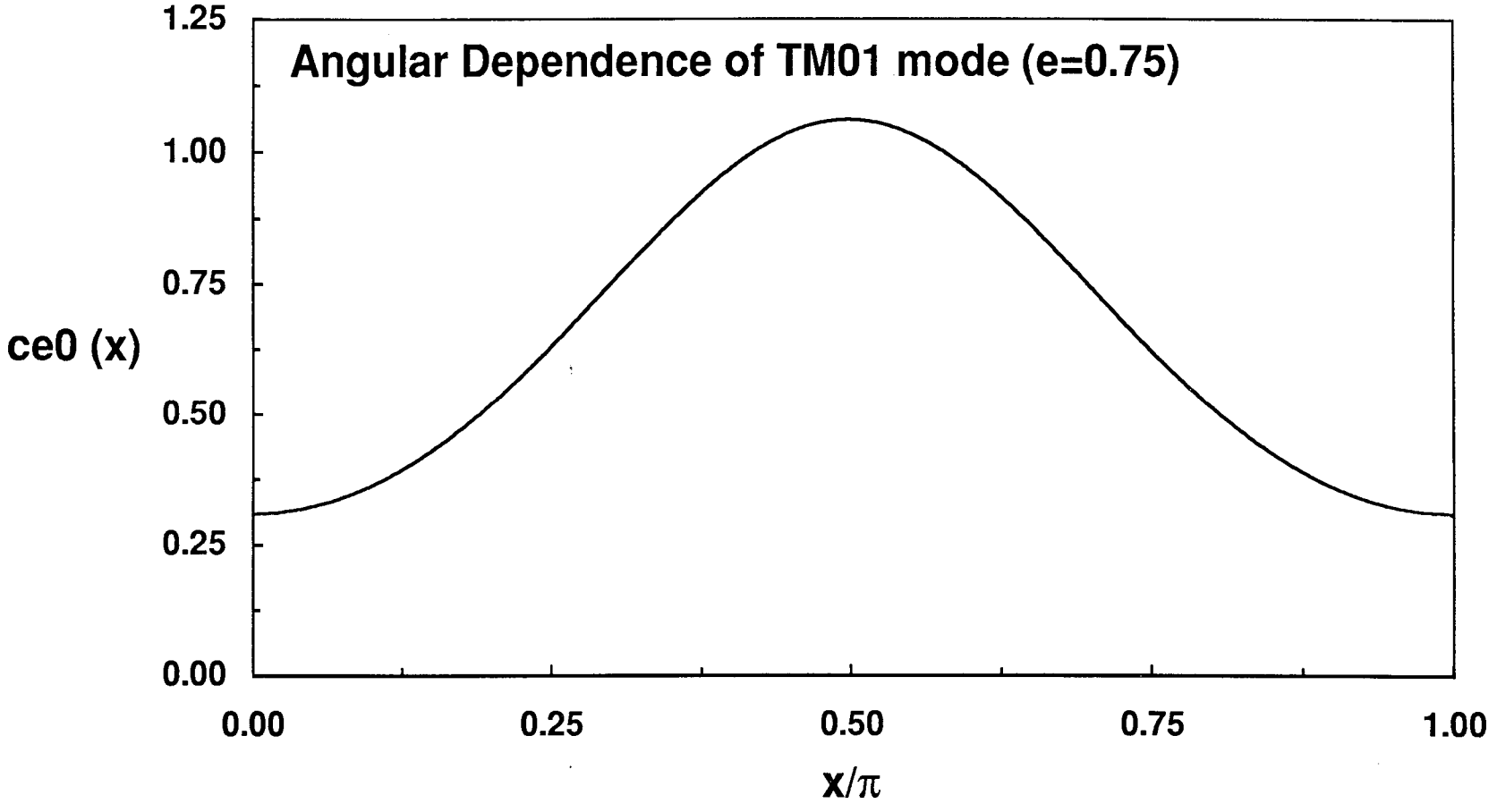
Angular Dependence of TM01 mode (e=0.75)
ce0 (x)
1.25
1.00
0.75
0.50
0.25
0.00
0.00
0.25
0.50
0.75
1.00
x/π

Figure 3

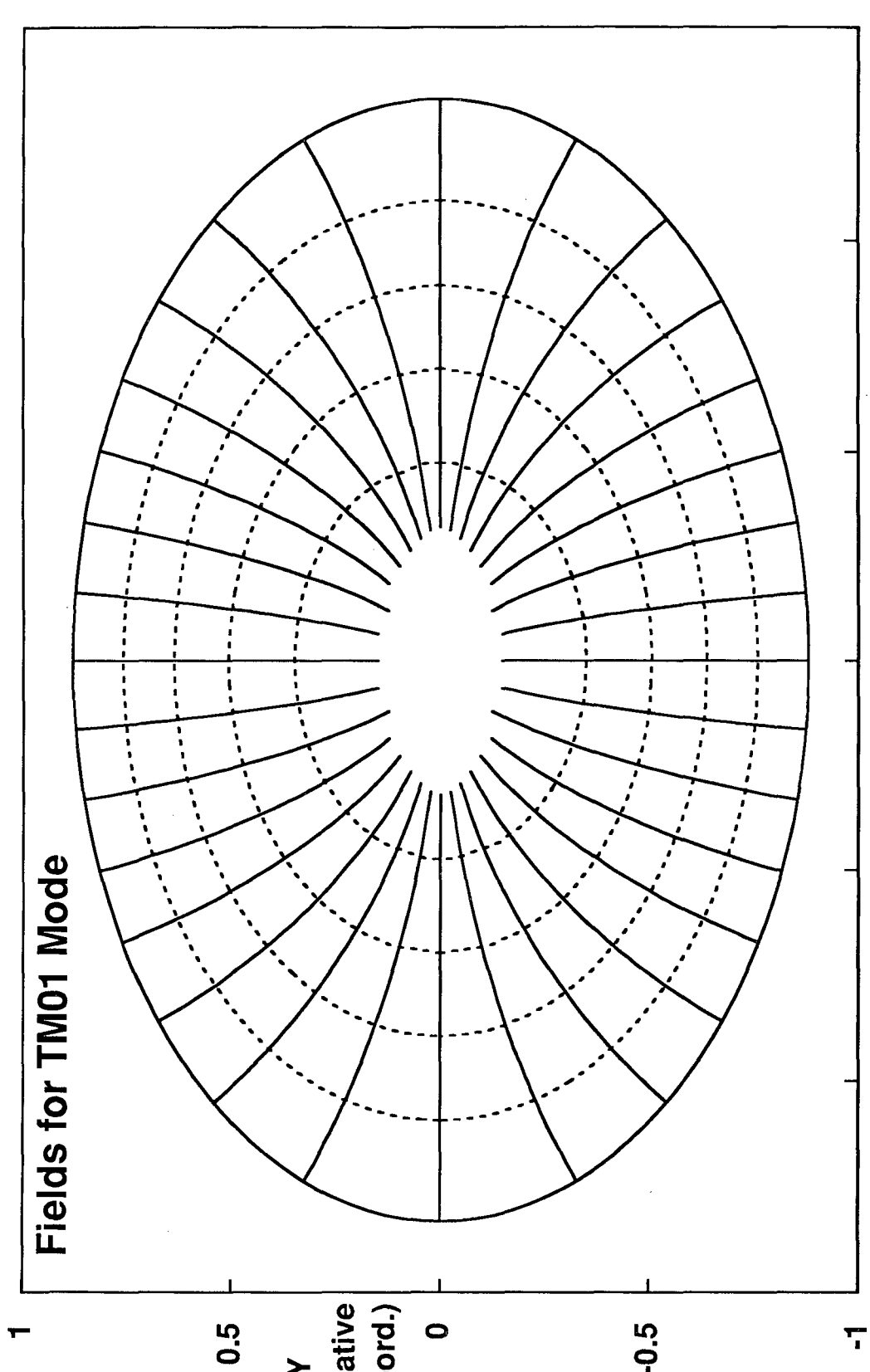
Fields for TM01 Mode
Y (Relative Coord.)
X (Relative Coordinate)
1
0.5
0
-0.5
-1
-1.5
-1
-0.5
0
0.5
1
1.5

Figure 4

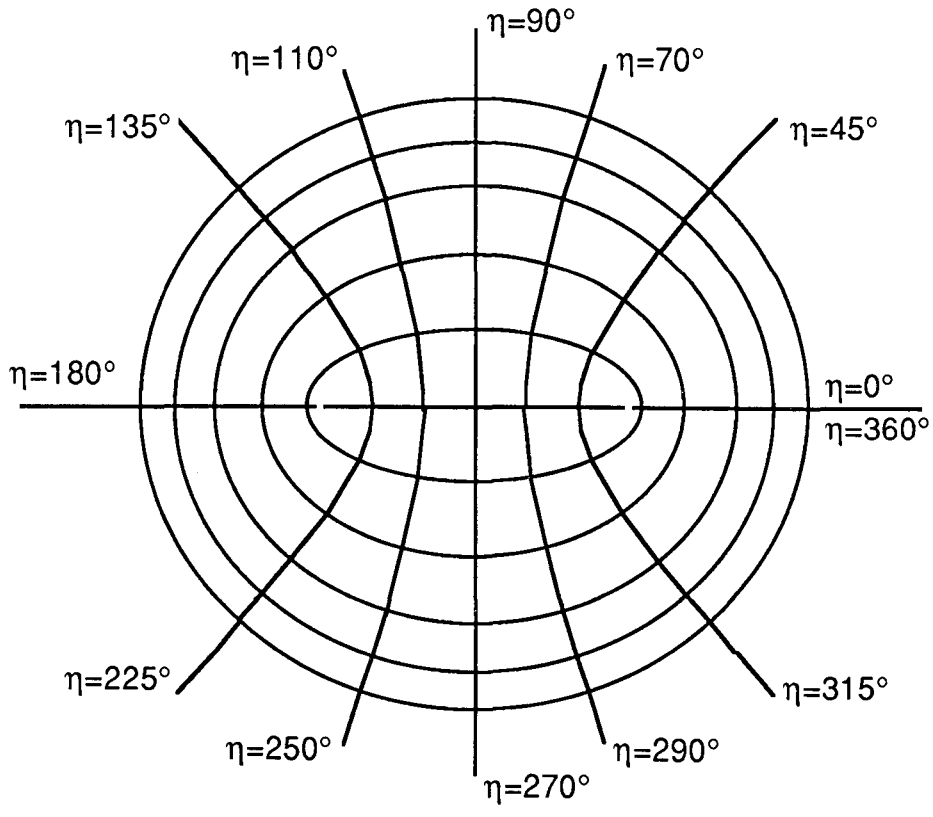

Figure A.1

LAWRENCE BERKELEY LABORATORY
UNIVERSITY OF CALIFORNIA
INFORMATION RESOURCES DEPARTMENT
1 CYCLOTRON ROAD
BERKELEY, CALIFORNIA 94720